

DRAFT VERSION FEBRUARY 13, 2025  
Typeset using L<sup>A</sup>T<sub>E</sub>X default style in AASTeX631

## Markarian 501 reincarnates with vigor as a temporary EHL during VHE flaring in July 2014

SARIRA SAHU,<sup>1</sup> A. U. PUGA OLIVEROS,<sup>1</sup> D. I. PÁEZ-SÁNCHEZ,<sup>1</sup> G. SÁNCHEZ-COLÓN,<sup>2</sup> SUBHASH RAJPOOT,<sup>3</sup>  
M. E. IGLESIAS MARTÍNEZ,<sup>4</sup> JOSE GUERRA CARMENATE,<sup>4</sup> P. FERNÁNDEZ DE CÓRDOBA,<sup>4</sup> AND GAETANO LAMBIASE<sup>5,6</sup>

<sup>1</sup>*Instituto de Ciencias Nucleares, Universidad Nacional Autónoma de México,  
Circuito Exterior S/N, C.U., A. Postal 70-543, CDMX 04510, México.*

<sup>2</sup>*Departamento de Física Aplicada, Centro de Investigación y de Estudios Avanzados del IPN,  
Unidad Mérida. A. Postal 73, Cordemex, Mérida, Yucatán 97310, México.*

<sup>3</sup>*Department of Physics and Astronomy, California State University,  
1250 Bellflower Boulevard, Long Beach, CA 90840, USA.*

<sup>4</sup>*Instituto Universitario de Matemática Pura y Aplicada,  
Universitat Politècnica de València, Camino de Vera s/n, 46022 Valencia, Spain*

<sup>5</sup>*Dipartimento di Fisica “E.R. Caianiello”, Università di Salerno, Via Giovanni Paolo II, I-84084 Fisciano (SA), Italy*

<sup>6</sup>*INFN, Gruppo collegato di Salerno, Via Giovanni Paolo II, I-84084 Fisciano (SA), Italy*

### ABSTRACT

Markarian 501, a well known high energy BL Lac object, has exhibited several epochs of very high energy (VHE) gamma-ray flaring events when its synchrotron peak frequency shifted above  $10^{17}$  Hz, a signature of extreme behavior. From July 16 to July 31, 2014 such flaring events were observed for 15 days by various telescopes. On July 19 (MJD 56857.98), the X-ray outburst from the source was at its highest and on the same day an intriguing narrow peak-like feature around 3 TeV was observed by MAGIC telescopes, a feature inconsistent with standard interpretations. Using the well known two-zone photohadronic model, we study these VHE gamma-ray spectra on a day-by-day basis and offer explanation. Our two-zone photohadronic scenario shows that, on MJD 56857.98, the peak-like feature appears at a cutoff energy of  $E_{\gamma}^c = 3.18$  TeV. Below this energy the observed VHE spectrum increases slowly and above  $E_{\gamma}^c$  it falls faster, thus resulting in a mild peak-like feature.

*Keywords:* High energy astrophysics (739), Blazars (164), Gamma-rays (637), Relativistic jets (1390), BL Lacertae objects (158)

### 1. INTRODUCTION

Markarian 501 (Mrk 501) is a high synchrotron peaked BL Lac object (HBL) at a redshift of  $z = 0.034$  (Ulrich et al. 1975). It is the second well known bright HBL after Markarian 421 (Mrk 421) and is one of the brightest extragalactic

sarira@nucleares.unam.mx

angel.puga@correo.nucleares.unam.mx

diana.paez@correo.nucleares.unam.mx

gabriel.sanchez@cinvestav.mx

Subhash.Rajpoot@csulb.edu

miigmar@upv.es

jguecar@doctor.upv.es

pfernandez@mat.upv.es

lambiase@sa.infn.it

sources in the X-ray/TeV sky. Since its discovery in VHE by Whipple telescopes in 1996 (Abdo et al. 2009), several major outburst in multi-TeV have been observed and has been the target of many multiwavelength campaigns mainly covering VHE flaring activities (Kataoka et al. 1999; Albert et al. 2008; Kranich 2009; Aleksić et al. 2015). Mrk 501 is one of the few blazars which can be monitored even during the low emission periods. To understand different emission mechanisms and their characterizations, it is essential to have long-term and multiwavelength observations of the spectral energy distribution (SED) of the blazars. Also, simultaneous correlation studies in different wavelengths of the SED during the flaring can help us to constrain the emission mechanisms. Motivated by these goals, several multi-wavelength and multi-instrument observation campaigns were organized. In 1997, from March to October, Mrk 501 had an unprecedented flare in VHE gamma-rays and the integral flux reached up to four times the magnitude of the Crab Nebula (CU) flux (Petry et al. 2000). Also, it was extremely active in the X-ray region during this period and the synchrotron peak had a dramatic shift to energies above 100 keV, which is more than two orders of magnitude compared to that of the typical non-flaring state.

During May to July 2005, Major Atmospheric Gamma-Ray Imaging Cherenkov (MAGIC) telescopes made observations for 30 nights and flaring above 100 GeV was observed with an order of magnitude flux variation (Albert et al. 2007). On the nights of June 30 and July 9, flux-doubling in VHE band was observed within a time span of about 2 minutes. This is the fastest flux variation ever observed from Mrk 501 since its discovery. During this observation period, the synchrotron peak and the VHE peak were shifted towards higher energy limits. As a part of the long term multiwavelength campaign, Mrk 501 was observed by  $\sim 30$  different instruments and covered the entire electromagnetic spectrum (Aliu et al. 2016; Ahnen et al. 2017) from March 15 to August 1, 2009.

Between March and July of 2012, another multiwavelength campaign was undertaken when more than 25 different telescopes, including MAGIC, and Very Energetic Radiation Imaging Telescope Array System (VERITAS), took part and fluxes above 0.2 TeV were observed (Ahnen et al. 2018). The highest peak flux was recorded on June 9, and most importantly, the X-ray spectrum and the VHE gamma-ray spectrum were observed to be extremely hard. During this period the synchrotron peak was above 5 keV and the Synchrotron Self-Compton (SSC) peak was above 0.5 TeV. The TeV Atmospheric Cherenkov Telescope with Imaging Camera (TACTIC) at Mt Abu, Rajasthan, India, observed Mrk 501 from 15 April to 30 May, 2012 at energies above 850 GeV energy for 70.6 h. Between 22 to 27 May, 2012, TACTIC telescope observed relatively high VHE flux in the energy range between 850 GeV and 17.24 TeV (Chandra et al. 2017).

Mrk 501 was monitored in the year 2014 with the First G-APD Cherenkov Telescope (FACT) (Anderhub et al. 2013; Biland et al. 2014; Dorner et al. 2015). Several high flaring states were observed. This triggered the HESS telescopes to undertake further observations. Enhanced VHE gamma-ray flux, comparable to the exceptional flare of 1997, was observed on the night of June 23-24, 2014 (MJD 56832) with the HESS phase-II telescopes. The energy of the VHE photons extended up to 20 TeV and the flux had a rapid variability. Estimates indicate that this is the highest flux ever observed from Mrk 501 with the HESS telescopes (Abdalla et al. 2019).

Again, in July of 2014, flaring in X-ray and VHE gamma-ray were observed for about two weeks (from 16th to 31st) by the MAGIC telescopes (MAGIC Collaboration et al. 2020). The X-ray flaring was found to be exceptionally high, similar to the historic 1997 flaring. This amounts to the largest flux ever detected so far with the X-ray Telescope (XRT) on board the Neil Gehrels Swift Gamma-ray Burst Observatory (Gehrels et al. 2004) in its operational history. Also, the VHE gamma-ray emission above 0.15 TeV during this time was high, about 0.5 to 2 times of the Crab nebula flux. On July 19 (MJD 56857.98), the day of the highest X-ray activity, a narrow peak-like feature at  $\sim 3$  TeV was observed by MAGIC telescopes (MAGIC Collaboration et al. 2020).

In the Universe, the most dominant sources of extragalactic  $\gamma$ -rays are the blazars (Romero et al. 2017). Their SED is characterized by two non-thermal peaks (Abdo et al. 2010), the synchrotron peak is in the infrared to X-ray frequency range and the SSC peak is in the X-ray to gamma-ray range. The BL Lac objects belong to the blazar family and are classified according to the position of their synchrotron peak frequency  $\nu_s^p$  in the SED. The classification list is as, low-energy peaked blazars (LBLs,  $\nu_s^p < 10^{14}$  Hz), intermediate-energy peaked blazars (IBLs,  $10^{14}$  Hz  $< \nu_s^p < 10^{15}$  Hz), high-energy peaked blazars (HBLs,  $10^{15}$  Hz  $< \nu_s^p < 10^{17}$  Hz (Padovani & Giommi 1995; Abdo et al. 2010; Boettcher et al. 2013)) and extreme high-energy peaked blazars (EHBLs,  $\nu_s^p > 10^{17}$  Hz (Costamante et al. 2001)) with extreme spectral properties.

Low luminosity and limited variability of EHBLs hinder the detection of their gamma-rays by the current generation Imaging Atmospheric Cerenkov Telescopes (IACTs). Thus, only a handful number of EHBLs have been detected so far and well known among them are 1ES 0229+200, 1ES 0347-232, RGB J0710+591 and 1ES 1101-232 (Costamante et al.

2018). It is observed that, at least three nearby extensively studied HBLs, Mrk 421, Mrk 501 and 1ES 1959+650 have shown temporary EHBL (tEHBL) like behavior during several flaring epochs (Sahu et al. 2020; Sahu et al. 2021a,b). During tEHBL-like behavior, the synchrotron peaks have shifted above  $10^{17}$  Hz and the TeV spectra are harder. Also, due to the complex behavior of these sources with different spectral properties at VHE gamma-rays, the possibility of different sub-classes within the EHBL class can not be ruled out (Foffano et al. 2019).

With the standard one-zone leptonic SSC model, it is difficult to explain the VHE spectrum of EHBL, since the leptonic model predicts softer SSC spectrum in the Klein-Nishina regime, and is contrary to observations (Paggi et al. 2009). However, one can circumvent this problem by adopting unrealistic parameters, such as, large bulk Lorentz factor, large electron Lorentz factor and a small magnetic field (Ahnen et al. 2018; Acciari et al. 2020). Alternative solutions are also proposed, such as: the two-zone leptonic model, Inverse Compton scattering of the electrons with the cosmic microwave background, the spine-layer structured jet model and different hadronic models (Böttcher et al. 2008; Acciari et al. 2019; Ahnen et al. 2018).

VHE gamma-rays from the extragalactic sources get attenuated by interacting with the extragalactic background light (EBL) and this attenuation is energy dependent. The shape of the observed spectrum changes at very high energies, so, EBL corrections to the observed spectrum have to be taken care of (Franceschini et al. 2008; Dominguez et al. 2011; Tavecchio 2014; Tavecchio & Bonnoli 2015). EHBLs have extreme spectral properties in TeV energy range, and probably these are ideal probes for EBL.

The multiwavelength SED of the HBL, Mrk 501, during several flaring periods are explained well using the leptonic models and hadronic models (Böttcher et al. 2008; Acciari et al. 2019; Ahnen et al. 2018; Sahu 2019; Sahu et al. 2020). However, Mrk 501 had VHE flaring during 2005 and 2012 when the synchrotron peak had shifted above 1 keV, clearly a signature of EHBL-like behavior. In the context of leptonic model, explaining such shift and simultaneously explaining the VHE flaring event is problematic. We have used the two-zone photohadronic model to explain the tEHBL-like behavior of these flaring events very well. We show that the photon background in the low energy tail region of the SSC spectrum is not a single power-law as in the case of HBLs, but consists of two power-laws, separating it in to two different zones. Similarly, the extensively studied nearby HBLs, Mrk 421 and 1ES 1959+650 have also shown tEHBL-like behavior occasionally, and using the two-zone photohadronic model, we have successfully explained their VHE flaring events. In this work our goal is to explain the VHE flaring events observed during July 16 to July 31, 2014, and particularly, to interpret the unusual peak-like feature at about 3 TeV observed on July 19 (MJD 56857.98) in the context of the two-zone photohadronic model.

The paper is organized as follows. In section 2, the two-zone photohadronic model is briefly discussed. In section 3, we discuss the flaring events of Mrk 501 during July 16 to July 31, 2014 (MJD 56854–56869). A detail analysis of the VHE events observed by MAGIC for about two weeks are discussed in section 4 and a brief discussion is given in section 5.

## 2. TWO-ZONE PHOTOHADRONIC MODEL

The photohadronic model is very successful in explaining the VHE spectra from several HBLs (Sahu et al. 2013; Sahu 2019; Sahu et al. 2019). This model is based on the fact that the low and high energy peaks of the blazar are produced from the synchrotron process of the electrons and inverse Compton scattering of electrons in the jet environment respectively (the leptonic model). The region where these photons are emitted is a blob of comoving radius  $R'_b$  (where ' implies comoving frame), with a bulk Lorentz factor  $\Gamma$  and a Doppler factor  $\mathcal{D}$ . For HBLs,  $\Gamma \simeq \mathcal{D}$ . In the photohadronic scenario, accelerated protons are injected in the jet with a differential spectrum  $dN/dE_p \propto E_p^{-\alpha}$ , where the spectral index  $\alpha \geq 2$  (Dermer & Schlickeiser 1993). These protons interact with the background seed photons to produce  $\Delta$ -resonances,  $p\gamma \rightarrow \Delta^+$ . Decay of the  $\Delta^+$  to neutral pion produces observed gamma-rays. The kinematical condition to produce  $\Delta^+$  is given by,

$$E_p \epsilon_\gamma = \frac{0.32 \Gamma^2}{(1+z)^2} \text{ GeV}^2, \quad (1)$$

where  $E_p$  and  $\epsilon_\gamma$  are respectively the observed proton energy, the seed photon energy and  $z$  is the redshift of the source. The energy of the observed gamma-ray  $E_\gamma$  from the  $\pi^0$  decay carries 10% of the original proton energy.

It is observed that in the standard jet scenario of the BL lac objects, the  $p\gamma \rightarrow \Delta^+$  process is inefficient due to the low background photon density (Pjanka et al. 2017). To void this problem in the photohadronic model we assume that during the VHE flaring of the source, an internal compact jet is formed within the larger jet (Sahu et al. 2016, 2018).

The inner jet has radius  $R'_f$  and the outer jet has radius  $R'_b$  and  $R'_f < R'_b$ . Also, the photon density in the inner jet region,  $n'_{\gamma,f}$ , is larger than the photon density in the outer jet region,  $n'_\gamma$  ( $n'_{\gamma,f} > n'_\gamma$ ). During the VHE flaring, the accelerated high energy protons interact with the seed photons in inner jet region to produce  $\Delta$ -resonance. Due to high density photons in the inner jet region, the efficiency of the production of  $\Delta$ -resonance is relatively high as compared to the standard jet scenario and this avoids the necessity for super-Eddington luminosity of protons.

The inner jet region is hidden and the photon density  $n'_{\gamma,f}$  is unknown. But the photon density in the outer jet region is known. Also, due to the adiabatic expansion of the inner jet, its photon density decreases when it crosses into the outer jet. To connect the inner and the outer region photon densities we assume a scaling relation given by (Sahu et al. 2019)

$$\frac{n'_{\gamma,f}(\epsilon_{\gamma,1})}{n'_{\gamma,f}(\epsilon_{\gamma,2})} \simeq \frac{n'_\gamma(\epsilon_{\gamma,1})}{n'_\gamma(\epsilon_{\gamma,2})}. \quad (2)$$

The above relation shows that during the multi-TeV gamma-ray flaring in a blazar, the ratios of the photon densities at energies  $\epsilon_{\gamma,1}$  and  $\epsilon_{\gamma,2}$  in the inner jet and the outer jet regions are almost the same. Thus, by using the relation in Eq. (2), we can express the unknown photon density in the inner jet region in terms of the observed photon density in the outer jet region.

From the previous analysis of the VHE spectra of dozens of HBLs in the photohadronic model, we observe that to produce the observed  $E_\gamma$ , the background seed photon energy  $\epsilon_\gamma$  always lies in the low energy tail region of the SSC spectrum and the SSC flux is a perfect power-law, given by  $\Phi_{SSC} \propto \epsilon_\gamma^\beta \propto E_\gamma^{-\beta}$ , with  $\beta$  the photon spectral index (Sahu 2019). Thus the observed GeV-TeV photon flux from a HBL is given as

$$F_{\gamma,obs}(E_\gamma) = F_0 \left( \frac{E_\gamma}{TeV} \right)^{-\delta+3} e^{-\tau_{\gamma\gamma}(E_\gamma,z)} = F_{\gamma,in}(E_\gamma) e^{-\tau_{\gamma\gamma}(E_\gamma,z)}. \quad (3)$$

In the above equation,  $F_0$  is the flux normalization,  $F_{\gamma,in}$  is the intrinsic VHE gamma-ray flux and the exponential factor corresponds to the survival probability of VHE photon due to its interaction with the EBL photons which has the optical depth  $\tau_{\gamma\gamma}$ . For the EBL correction to the VHE spectrum, here, we use the EBL model of Franceschini et al. (2008). The exponent  $\delta = \alpha + \beta$  and for HBLs, it is in the range  $2.5 \leq \delta \leq 3.0$ . From detail analysis of several VHE spectra of HBLs it was observed that the flaring states can be in three categories, viz, (i) very high emission state with  $2.5 \leq \delta \leq 2.6$ , (ii) high emission state with  $2.6 < \delta < 3.0$  and (iii) low emission state with  $\delta = 3.0$  (Sahu et al. 2019). But for a tEHBL spectrum, it was shown that the single power-law behavior of the form  $\Phi_{SSC} \propto E_\gamma^{-\beta}$  does not work. Thus, two power-laws for the background seed photons in the low energy tail region is assumed in the form (Sahu et al. 2020).

$$\Phi_{SSC} \propto \begin{cases} E_\gamma^{-\beta_1}, & 100 \text{ GeV} \lesssim E_\gamma \lesssim E_\gamma^c \\ E_\gamma^{-\beta_2}, & E_\gamma \gtrsim E_\gamma^c \end{cases}, \quad (4)$$

with the spectral indices  $\beta_1 \neq \beta_2$  ( $\beta_i > 0$ ) and  $E_\gamma^c$  is the cutoff energy scale around which the transition between zone-1 and zone-2 takes place. The value of  $E_\gamma^c$  is different for different spectra. Thus, using Eq.(4), the observed spectrum for a temporary EHBL can be expressed as

$$F_{\gamma,obs} = e^{-\tau_{\gamma\gamma}} \times \begin{cases} F_1 \left( \frac{E_\gamma}{TeV} \right)^{-\delta_1+3}, & 100 \text{ GeV} \lesssim E_\gamma \lesssim E_\gamma^c \text{ (zone-1)} \\ F_2 \left( \frac{E_\gamma}{TeV} \right)^{-\delta_2+3}, & E_\gamma \gtrsim E_\gamma^c \text{ (zone-2)} \end{cases}. \quad (5)$$

$F_1$  and  $F_2$  are the normalization constants and  $\delta_i = \alpha + \beta_i$  ( $i = 1, 2$ ) are the free parameters in the photohadronic model that are to be adjusted by fitting to the observed VHE spectrum. Previously, the study of tEHBL-like behavior of Mrk421, Mrk501 and 1ES1959+650 in the context of two-zone photohadronic model have shown  $2.5 \leq \delta_1 \leq 3.0$  and  $3.0 < \delta_2 \leq 3.5$  (Sahu et al. 2020; Sahu et al. 2021a,b).

### 3. VHE FLARING OF MARKARIAN 501 DURING 2014

Mrk 501 was observed in multiwavelength by various instruments from July 16 to 31, 2014. During this period MAGIC telescopes observed for 13.5 h under dark and good atmospheric conditions (MAGIC Collaboration et al. 2020). The X-ray activity observed by the *Neil Gehrels Swift* Gamma-ray Burst Observatory was at its highest during its operational history and the spectra observed by different X-ray telescopes were very hard, similar to the large

historic flare of 1997 when the synchrotron peak was shifted above 100 keV (Pian et al. 1998; Tavecchio et al. 2001), an indication of EHBL-like behavior. It is interesting to note that the flux variation during July 2014 in the energy regime covering the radio, optical and GeV energies was mild, but the enhanced emission in X-ray and VHE gamma-ray were significantly correlated ( $> 3\sigma$ ). Also, it was observed that the strength and the significance of the correlation increased for increasing energy in X-rays. For 0.3-2 keV the correlation was  $\sim 3\sigma$  and for 2-10 keV the correlation was  $\sim 4\sigma$  respectively. Temporal evaluation of the fluxes in X-ray and VHE gamma-ray were characterized on a day-by-day basis from July 16 to July 31, 2014 (MJD 56854–56869). Harder-when-brighter trends in X-ray spectra were observed, but the VHE spectra observed by MAGIC did not show such behavior. A summary of the VHE gamma-ray observations by MAGIC telescopes at different zenith angles is shown in Table 1 (MAGIC Collaboration et al. 2020).

During the X-ray outburst, it was observed that the VHE gamma-ray flux above 0.15 TeV varied from  $\sim 0.5$  to  $\sim 2$  times the CU flux and no intra-night variability was observed in VHE gamma-rays during this two weeks flaring period. On 2014 July 19 (MJD56857.98) the highest X-ray flux above 2 keV was recorded by *Swift* while the MAGIC telescopes observed a rare unusual narrow spectral feature at  $\sim 3$  TeV in the VHE spectrum. This intriguing peak-like feature is inconsistent with the standard analytic functions widely used to fit the VHE spectra of blazars. The observed broadband SED for 15 consecutive days, from July 16 to July 31, 2014, were explained using one-zone SSC models. Also, the narrow spectral feature on MJD 56857.98 is modeled by using the leptonic and the hadronic models (Hu & Yan 2021; Petropoulou et al. 2024).

**Table 1.** The VHE observations of Mrk 501 by MAGIC telescopes during July 16 to July 31, 2014 are summarized in the table. The fourth column corresponds to the range of the observed zenith angle and the fifth column corresponds to the significance of the observation MAGIC Collaboration et al. (2020).

Date	MJD	Obs. time[h]	Zd[°]	Significance
2014/07/16	56854.91	0.45	10–15	13.1 $\sigma$
2014/07/17	56855.91	0.37	11–14	15.9 $\sigma$
2014/07/18	56856.91	0.48	11–14	22.5 $\sigma$
2014/07/19	56857.98*	1.54	10–40	36.5 $\sigma$
2014/07/20	56858.98	0.63	10–41	27.9 $\sigma$
2014/07/21	56859.97	1.48	10–38	40.0 $\sigma$
2014/07/23	56861.01	0.49	24–32	16.6 $\sigma$
2014/07/24	56862.02	1.28	25–42	21.9 $\sigma$
2014/07/25	56863.00	0.49	25–32	17.8 $\sigma$
2014/07/26	56864.02	1.26	24–41	26.6 $\sigma$
2014/07/27	56865.00	0.44	25–32	17.4 $\sigma$
2014/07/28	56865.99	2.13	17–41	57.4 $\sigma$
2014/07/29	56867.00	0.49	27–33	21.1 $\sigma$
2014/07/30	56868.01	1.29	26–43	42.7 $\sigma$
2014/07/31	56869.93	0.66	11–18	19.2 $\sigma$

Notes: \* A peak-like feature observed around 3 TeV.

#### 4. RESULTS

The Mrk501 is an extensively studied HBL in multiwavelength since its discovery and its VHE spectra are well explained by leptonic and hadronic models. However, during its VHE flaring in the years 1997, 2005 and 2012, it was observed that the synchrotron peak and the SSC peak were shifted towards higher energies. The synchrotron peaks were much above  $10^{17}$  Hz, signaling that the emissions were temporary EHBL-like, thus presented difficulties to explain the VHE spectra using the leptonic model. Also, the standard photohadronic model was inadequate to explain these VHE SED. We use two-zone photohadronic model to explain these spectra well. The flaring of Mrk501 during July 2014 as shown in Table 1, had exactly the same behavior that of the flaring of 1997, 2005 and 2012, when the synchrotron peak was in the EHBL regime (above  $10^{17}$  Hz) and the X-ray outburst was correlated with the VHE emission. So, we employ the two-zone photohadronic model to explain these 15 VHE spectra (from July 16 to July 31) on a day-by-day basis. A narrow peak-like feature at  $\sim 3$  TeV was found for the first time on July 19, the day

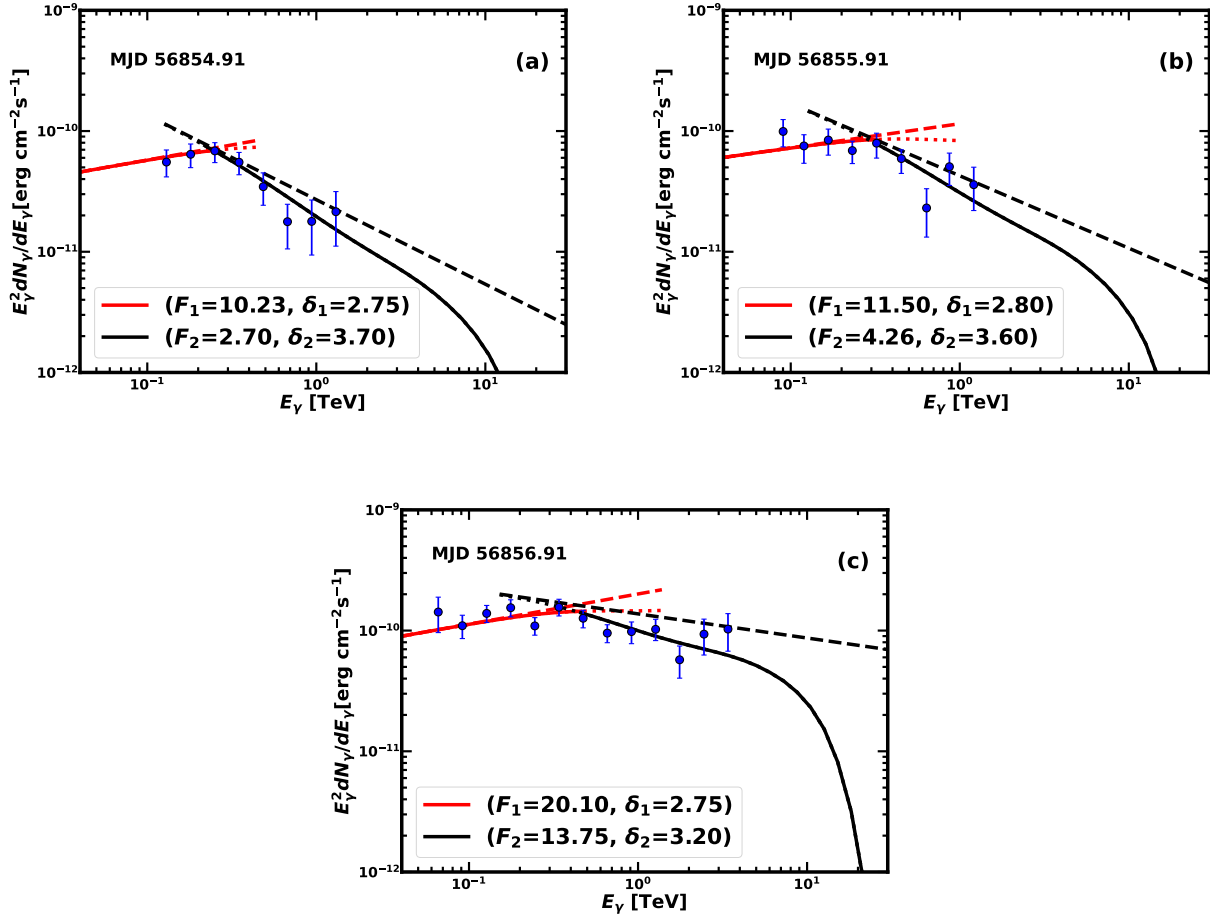


**Figure 1.** The observed VHE spectra of Mrk 501 for the first three days are fitted using the two-zone photohadronic model. In all the figures, the normalization constants  $F_1$  and  $F_2$  are expressed in units of  $10^{-11}$  erg cm $^{-2}$  s $^{-1}$ . The best fit to zone-1 is shown as the red curve and its extension as dotted red curve shows the behavior of the model at the high-energy limit if only zone-1 exists. Similarly, the spectrum in zone-2 is fitted with the black curve and the dashed black curve shows its behavior at the low-energy limit if only zone-2 exists. The dashed red and the dashed black curves are respectively the intrinsic curves corresponding to zone-1 and zone-2. The curves in Figures 2, 3, 4, and 5 have the same definitions and also, their normalization constants  $F_1$  and  $F_2$  are expressed in the same units as here.

when the highest X-ray flux was also observed. This feature is inconsistent with the traditional interpretation of VHE spectra by using the different analytic functions. We shall also discuss in detail this narrow peak-like feature.

There were hour time difference between the VHE gamma-ray observations and the X-ray observations during the 15 consecutive days. Six observations have temporal difference of less than 1 h, five observations have time difference between 1 and 2 h, two observations have 3 h time difference and remaining two VHE observations do not have X-ray observations. However, during these 15 days observation period, there was no significant intra-night variability in the X-ray and the VHE gamma-ray bands. So, one can assume that the X-ray and the VHE gamma-ray observations were simultaneous.

As stated above, the flaring of Mrk 501 during July 2014 was tEHBL-like, so, we shall use the two-zone photohadronic model to fit the VHE gamma-spectra. The VHE spectrum on MJD 56854.91 was observed in the energy range  $0.13 \text{ TeV} \leq E_\gamma \leq 1.3 \text{ TeV}$  and is fitted well with  $\delta_1 = 2.75$ ,  $F_1 = 10.23 \times 10^{-11}$  erg cm $^{-2}$  s $^{-1}$  for zone-1 and  $\delta_2 = 3.70$ ,  $F_2 = 2.70 \times 10^{-11}$  erg cm $^{-2}$  s $^{-1}$  for zone-2 as shown in Figure 1(a). The cutoff energy between zone-1 and zone-2 is  $E_\gamma^c = 0.25$  TeV. For zone-1,  $\delta_1 = 2.75$  corresponds to a high emission state and the intrinsic VHE photon flux  $F_{\gamma,in} \propto E_\gamma^{0.30}$ . But, for zone-2,  $F_{\gamma,in} \propto E_\gamma^{-0.70}$  which is consistent with the fast fall of the flux above  $E_\gamma^c$ . Also, our fits

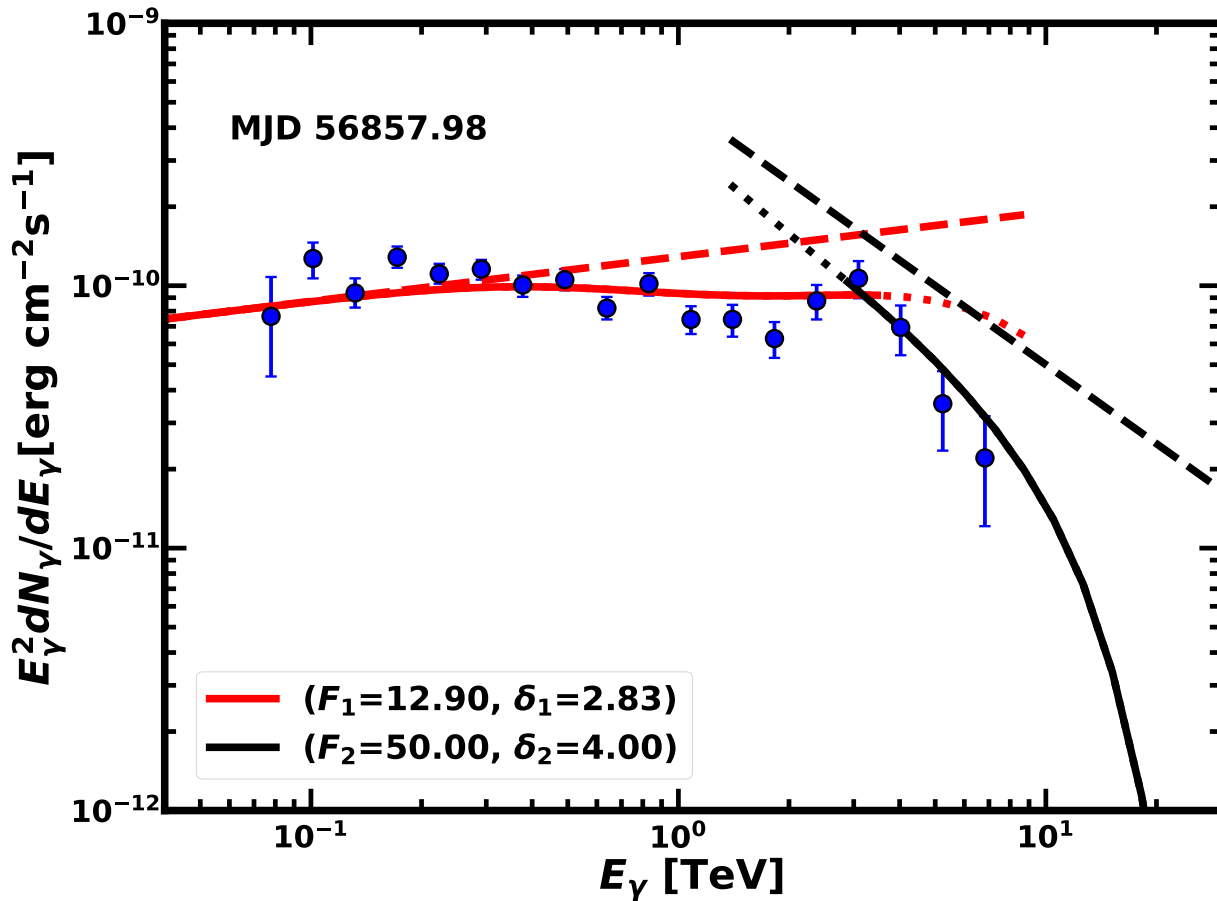


**Figure 2.** The VHE spectrum of Mrk 501 observed on MJD 56857.98. See Figure 1 for the definitions of the curves.

to both the zones are very good. Similarly, on MJD 56855.91, the best fit to the spectrum is obtained for  $\delta_1 = 2.80$ ,  $F_1 = 11.50 \times 10^{-11} \text{ erg cm}^{-2} \text{ s}^{-1}$  for zone-1 and  $\delta_2 = 3.60$ ,  $F_2 = 4.26 \times 10^{-11} \text{ erg cm}^{-2} \text{ s}^{-1}$  for zone-2 as shown in Figure 1(b). Here the cutoff energy  $E_\gamma^c = 0.29 \text{ TeV}$ , slightly higher than the previous day. On the third day (MJD 56856.91), the zone-1 is in high emission state with  $\delta_1 = 2.75$  and in zone-2, the flux decreases slower as compared to the previous day with  $\delta_2 = 3.20$  and  $E_\gamma^c = 0.43 \text{ TeV}$  (Figure 1(c)). It can be observed that  $E_\gamma^c$  has increased slowly from 0.25 TeV, from the first day to 0.43 TeV, to the third day.

A noticeable change in the spectrum on MJD 56857.98, on the fourth day was observed as shown in Figure 2. The spectrum was observed in the energy range  $0.08 \text{ TeV} \leq E_\gamma \leq 6.8 \text{ TeV}$ . Like previous days, zone-1 is still in the high emission state with  $\delta_1 = 2.83$ , but the cutoff energy drastically jumped to  $E_\gamma^c = 3.18 \text{ TeV}$ . Also, in zone-2, the spectrum falls extremely fast which can be fitted with  $\delta_2 = 4.0$ , which is shown in Figure 2. This is the first time we observe such a rapid fall of the VHE spectrum in zone-2 for tEHBL-like behavior of a HBL with a very large  $\delta_2$  value. Previously, we had studied the tEHBL-like behavior of Mrk 421, Mrk 501 and 1ES 1959+650 in different epochs using the two-zone photohadronic model, where we could explain the spectra very well and maximum value of  $\delta_2$  was 3.5 (Sahu et al. 2017, 2018, 2020; Sahu et al. 2021b). We had never observed such a fast fall of the spectrum in zone-2 and a cutoff energy very high. In this context, the VHE spectrum of Mrk 501 on MJD 56857.98 is unique and probably first of its type. Contrary to the claim by the MAGIC collaboration, our model does not predict a prominent peak at  $E_\gamma^c = 3.18 \text{ TeV}$ . We observe that the peak-like feature around  $E_\gamma^c$  is due to the slight increase in the flux in zone-1 and then a rapid fall of the spectrum for  $E_\gamma > E_\gamma^c$ .

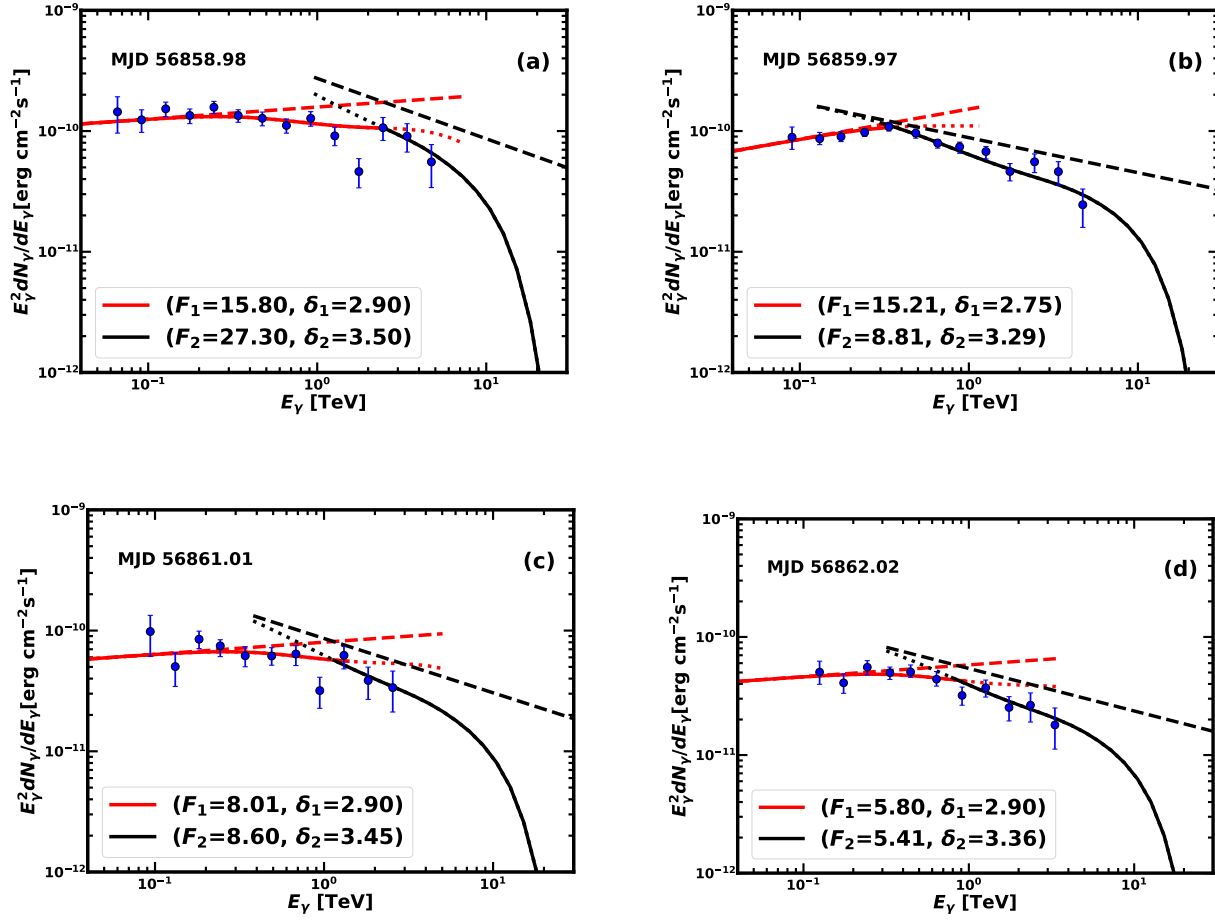


**Figure 3.** The observed VHE spectra on MJD 56859.98, 56859.97, 56861.01 and 56862.02 are fitted with the two-zone photo-hadronic model. See Figure 1 for the definitions of the curves.

The VHE spectra from July 20 to July 24 (MJD 56858.98 to MJD 56862.02) are fitted very well which are shown in Figure 3. It can be seen that, the spectral index  $\delta_1$  in zone-1 is always in the range  $2.6 < \delta_1 < 3.0$ , corresponding to a high emission state. Also, in zone-2 we have  $3.0 < \delta_2 \leq 3.5$  as observed in previous analysis to the VHE spectra of tEHBL-like behavior of several sources, including Mrk 501. On MJD 56858.98, the  $E_\gamma^c = 2.49$  TeV is high but the spectrum in zone-2 does not fall rapidly. So, we do not see any peak-like structure. On July 21 (MJD 56859.97), the cutoff energy drops down to very low,  $E_\gamma^c = 0.36$  TeV.

From July 25 to July 28 (MJD 56863.00 to MJD 56865.99), the spectra are fitted extremely well which are shown in Figure 4 with their respective parameters  $F_1$ ,  $F_2$ ,  $\delta_1$  and  $\delta_2$ . Throughout the observation period, the maximum VHE photon energy observed is on MJD 56865.99, which is  $E_\gamma = 15.1$  TeV. In Figure 5, the VHE spectra of MJD 56867.00 to MJD 56869.93 (July 29 to July 31) are shown with their respective parameters. Here also, the spectra are fitted very well. On July 31, again the cutoff energy  $E_\gamma^c = 2.38$ , which is high. However, the spectrum in zone-2 falls smoothly.

We have shown the best fit values of  $E_\gamma^c$  for all the 15 days observations in Figure 6. It can be seen that for the flaring on MJD 56857.98, the  $E_c$  is the maximum and on next day it decreases slightly and then a free fall on MJD 56859.97 to  $E_\gamma^c = 0.36$  TeV. Also, we observe an oscillating behavior in the  $E_\gamma^c$  values, which can be seen in Figure 6. Similarly, we have shown the best fit values of the VHE photon spectral indices  $\delta_1$  and  $\delta_2$  for zone-1 and zone-2 respectively in Figure 7. As the spectra in zone-1 are in high emission states, the values of  $\delta_1$  are very similar for the

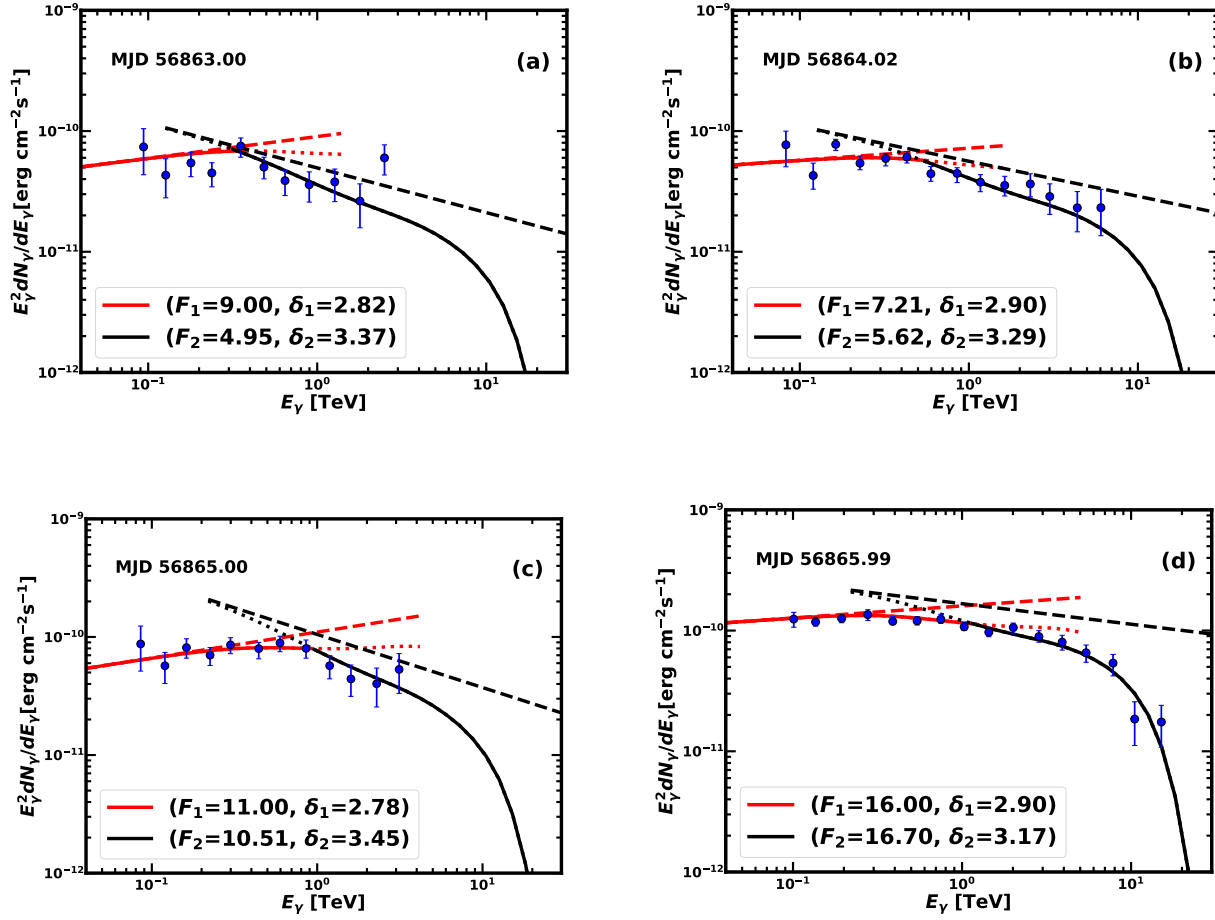


**Figure 4.** The VHE spectra observed on MJD 56863.00, 56864.02, 56865.00 and 56865.99 are fitted with the two-zone photohadronic model. See Figure 1 for the definitions of the curves.

whole period. However, in zone-2, we observe a variation in  $\delta_2$  and again the largest value of  $\delta_2 = 4.0$  is on MJD 56857.98.

In Figure 8, the best fit values of the normalization factors  $F_1$  and  $F_2$  are plotted for the whole observation period. It can be seen that the variation in  $F_1$  is minimal, however, there is a large variation in  $F_2$  and again, on MJD 56857.98, the variation is the highest. These analysis clearly show that the VHE spectrum of MJD 56857.98 is very distinct from the rest.

In the photohadronic model, high energy gamma-rays are produced from the interaction of high energy protons with the background SSC seed photons in the blazar jet. The region of the SSC flux responsible to produce the observed VHE gamma-rays lies in the low-energy tail region of the SSC spectrum which satisfies the condition in Eq. (1). For tEHBL-like behavior of an HBL, the VHE gamma-rays in zone-2 are produced when the accelerated high energy protons in the jet interact with the low energy MeV photons in the tail region of the SSC spectrum. The SSC flux in this region is  $\Phi_{SSC} \propto \epsilon_\gamma^{\beta_2} \propto E_\gamma^{-\beta_2}$ . Similarly, the SSC photon flux in zone-1 will behave as  $\Phi_{SSC} \propto \epsilon_\gamma^{\beta_1} \propto E_\gamma^{-\beta_1}$ . On MJD 56857.98, the best fit to zone-2 is achieved for  $\delta_2 = 4.0$ . With such a large  $\delta_2$ , the spectrum above  $E_\gamma^c = 3.18$  TeV falls rapidly. On this day, the highest energy photon observed is  $E_\gamma = 6.8$  TeV. This photon will be produced from the interaction of 68 TeV proton ( $10 E_\gamma$ ) with the SSC seed photon in the low energy tail region. Assuming that this seed photon has minimum energy  $\epsilon_\gamma \simeq 7.5 \times 10^{20}$  Hz ( $\sim 3.1$  MeV) (MAGIC Collaboration et al. 2020), the minimum bulk Lorentz factor is found to be  $\Gamma \simeq 26.5$ , which is consistent with the expectation. Using this  $\Gamma$  we can estimate the  $\epsilon_\gamma^c$  corresponding to the cutoff energy  $E_\gamma^c = 3.18$  TeV, which gives  $\epsilon_\gamma^c \sim 6.6$  MeV. By adopting the proton spectral

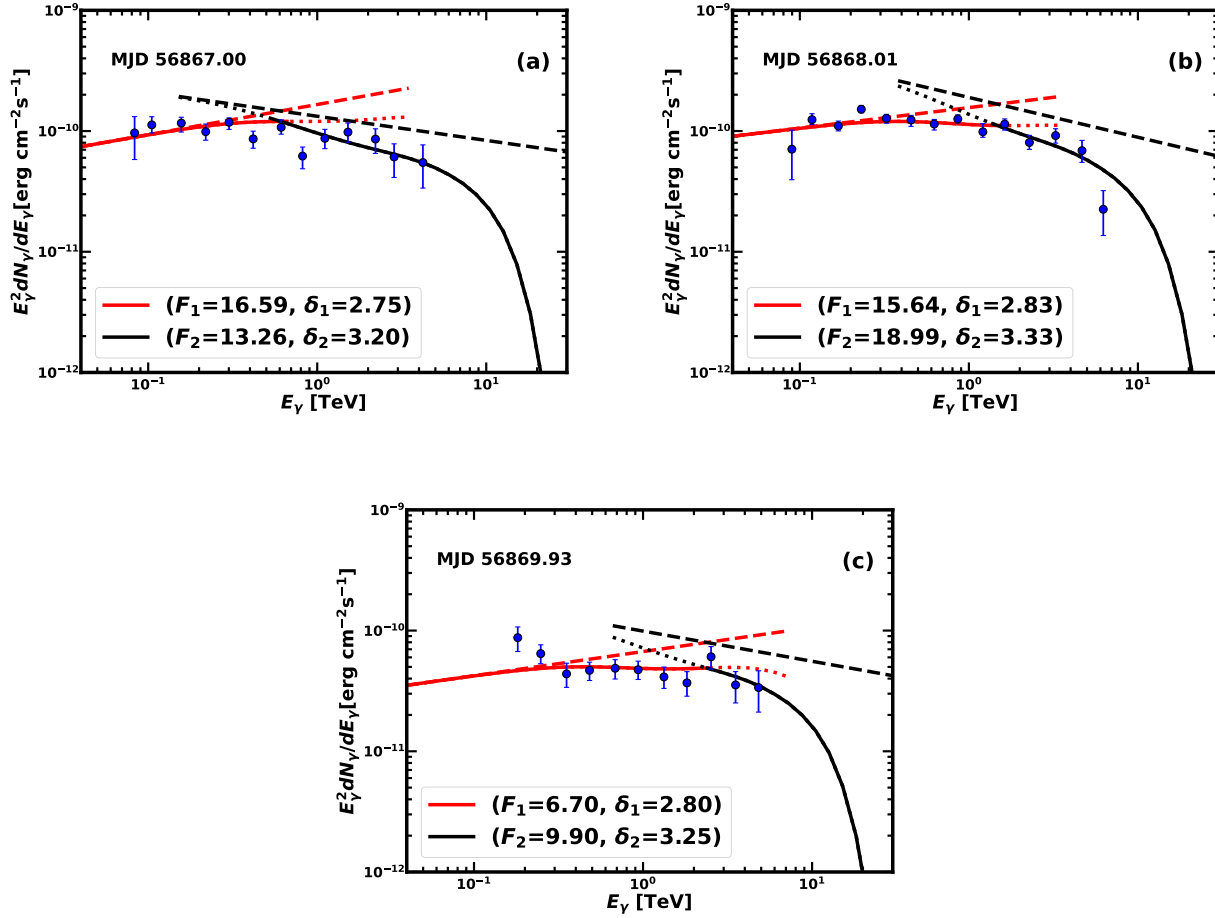


**Figure 5.** The observed VHE spectra on MJD 56867.00, 56868.01, and 56869.93 are fitted with the two-zone photohadronic model. See Figure 1 for the definitions of the curves.

index  $\alpha = 2.0$  (Dermer & Schlickeiser 1993), we get  $\beta_2 = 2.0$  and  $\beta_1 = 0.83$ . The low energy tail region of the SSC flux (zone-2) behaves as  $\Phi_{SSC} \propto \epsilon_\gamma^2$  in the energy range  $3.1 \text{ MeV} \lesssim \epsilon_\gamma \lesssim 6.6 \text{ MeV}$  and for  $\epsilon_\gamma \gtrsim 6.6 \text{ MeV}$  but in zone-1,  $\Phi_{SSC} \propto \epsilon_\gamma^{0.83}$ . The increase of  $\Phi_{SSC}$  is quadratic as a function of the seed photon energy  $\epsilon_\gamma$  in zone-2 and implies that the intrinsic VHE flux falls as  $F_{\gamma,in} \propto E_\gamma^{-\alpha-\beta_2+3} \propto E_\gamma^{-1}$ . Similarly, in zone-1, the intrinsic flux increases mildly as  $F_{\gamma,in} \propto E_\gamma^{0.17}$ .

#### 4.1. Comparison with flaring events of 2005 and 2012

The spectral analysis of the VHE flaring events during July 16 to July 31, 2014 (total 15 days) shows that the flaring events in zone-1 were in high emission states like a standard HBL spectrum which we have studied previously. Also, the spectra in zone-1 are very similar to the flaring events of Mrk 501 observed during 2005 May-July and 2012 June (Sahu et al. 2020). Similar spectra were also observed from Mrk 421 in 2010 March (Sahu et al. 2021b). However, we observed a large variation in the VHE spectra of Mrk 501 in zone-2 during 2014 flaring event, particularly on July 19, 2014 (MAGIC Collaboration et al. 2020). On this day, the spectral index  $\delta_2 = 4.0$  was observed to be very large, corresponding to a sharp fall in the VHE gamma-ray spectrum above a large cutoff energy  $E_\gamma^c = 3.18 \text{ TeV}$ .

During previous flaring events of Mrk 501 in 2005 and 2012, we did observe a variation in the spectra in zone-2,  $3.1 \lesssim \delta_2 \lesssim 3.5$ . However, this time the variation was observed to be abrupt. For example, on MJD 56856.91, the  $E_\gamma^c = 0.43 \text{ TeV}$  and  $\delta_2 = 3.2$  and on next day MJD 56857.98 it jumped to  $3.18 \text{ TeV}$  and  $4.0$  respectively. Such large values were not seen before in any of the tEHBL flaring events. On this day, the intrinsic flux in zone-1 increased as  $E_\gamma^{0.17}$  and decreased as  $E_\gamma^{-1}$  in zone-2. Thus, at  $E_\gamma^c = 3.18 \text{ TeV}$  there is a peak-like structure in the intrinsic spectrum

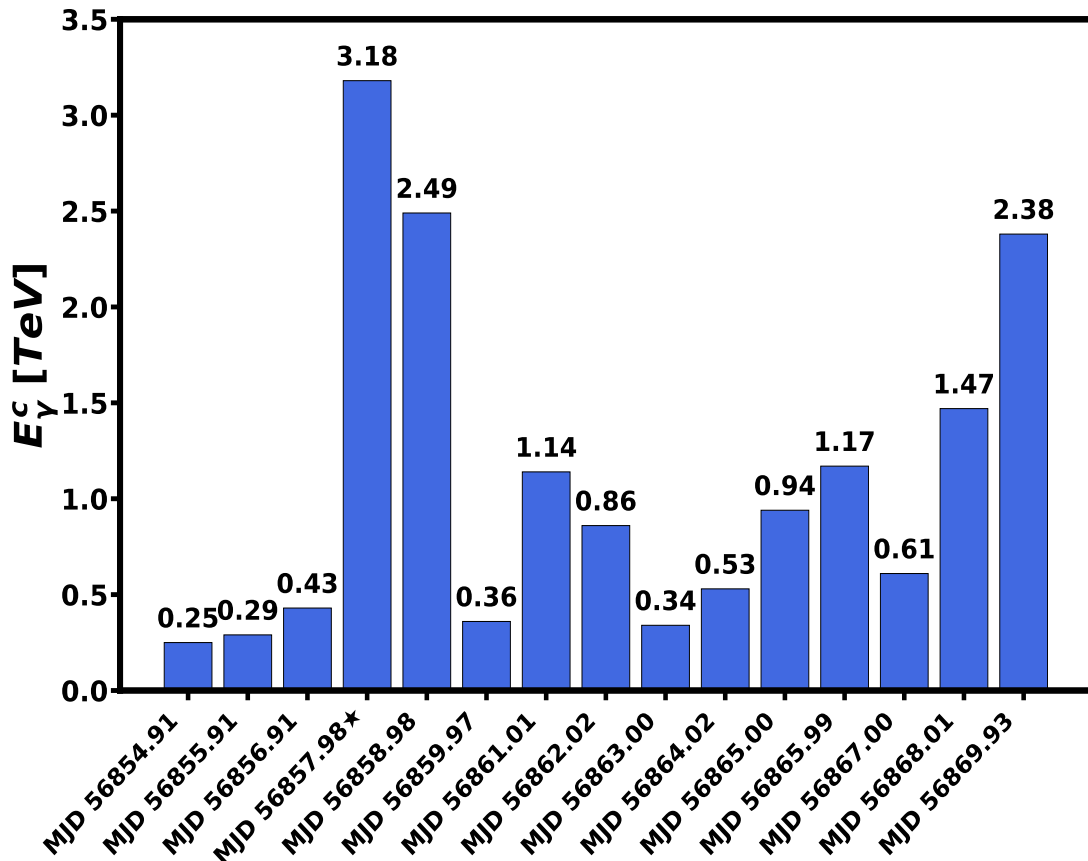


**Figure 6.** The cutoff energy  $E_{\gamma}^c$  in the two-zone photohadronic model is shown for every flaring event. MJD 56857.98\* corresponds to the day when a narrow peak-like feature at 3.18 TeV was observed and this is also shown in Figure 7, and in Figure 8.

but manifests as a milder peak in the observed spectrum due to EBL smoothing effect. As the spectral indices  $\beta_1$  and  $\beta_2$  are the distribution of the background seed photons in zone-1 and zone-2 respectively, the tEHBL-like behavior of Mrk 501 must be attributed to SSC band where  $\beta_2 = 2.0$  (zone-2). Previously, it was shown that the leptonic modeling of many HBL SEDs have deep valleys at the junction of synchrotron spectrum and the SSC spectrum with large  $\beta$  value (Sahu et al. 2017, 2018, 2020; Sahu et al. 2021b). It is possible that during these extreme flaring events, the inverse Compton scattering of high energy electrons with the self-produced synchrotron photons produces SSC photons in the narrow energy range of  $3.1 \text{ MeV} \lesssim \epsilon_{\gamma} \lesssim 6.6 \text{ MeV}$  (zone-2), which are piled up and the flux behaves as  $\Phi_{SSC} \propto \epsilon_{\gamma}^2$ .

## 5. DISCUSSION

Mrk 501 is a HBL which is extensively studied in all wavelenghts. Both leptonic models and hadronic models explain its spectra well. But the VHE emission during 2005, 2012 and 2014, when the synchrotron peak had shifted to frequencies above  $10^{17}$  Hz, the VHE spectra were difficult to explain. Actually, during these flaring periods, Mrk 501 behaved like temporary EHBL and its spectra were complex. Similar tEHBL-like behavior were also observed from Mrk 421 and 1ES 1959+650. In previous studies, we used the two-zone photohadronic model and explained very well the tEHBL-like behavior of these sources. In the present work we have used the two-zone photohadronic model again to explain the tEHBL-like behavior of Mrk 501 for the 15 days during July 16 to 31, 2014. It is observed that the spectra in zone-1 were like standard HBL and were in high emission states implying that the spectral indices in this region were in the range  $2.6 < \delta_1 < 3.0$ . During the VHE flaring period of 2005 and 2012 in Mrk 501, this same behavior was observed. However, the spectral behavior in zone-2 of the flaring in 2014 is much more complex and different than in the previous periods. Of particular importance is the VHE flaring event on MJD 56857.98 (July 19, 2014), when the cutoff energy  $E_{\gamma}^c = 3.18$  TeV and the spectral index in zone-2 was  $\delta_2 = 4.0$ . This high value of  $\delta_2$  implies that

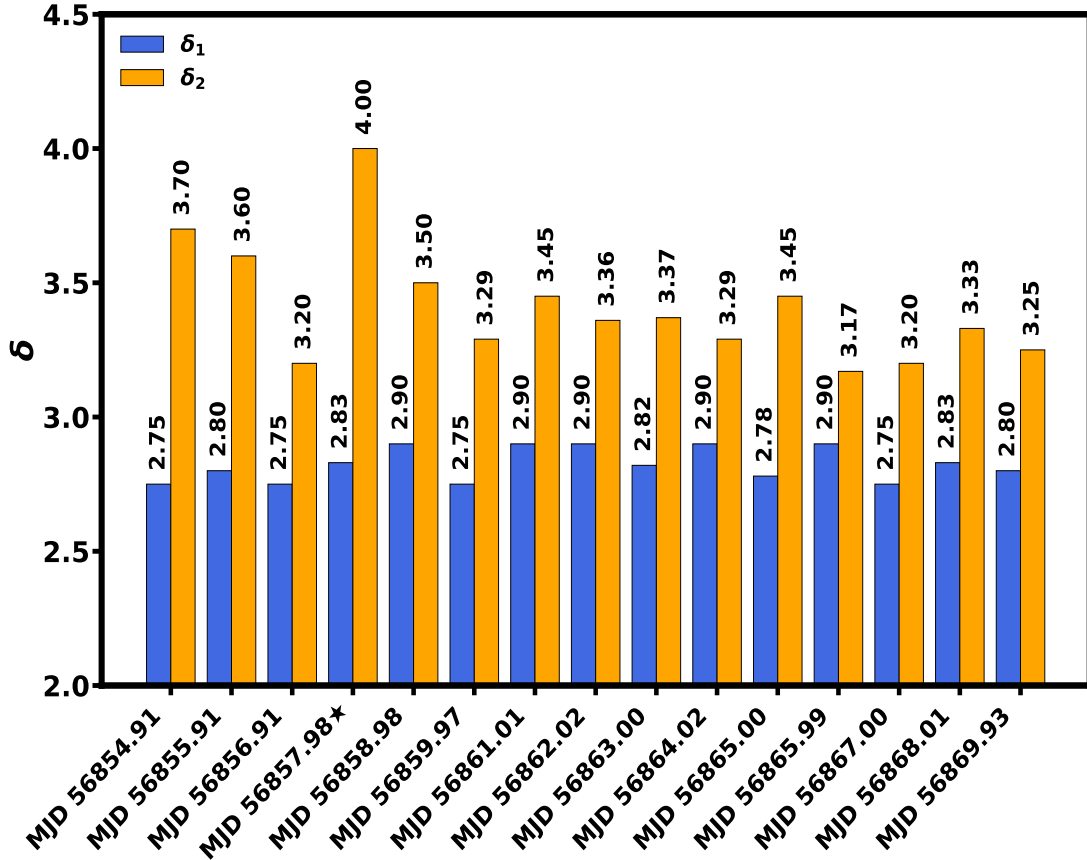


Figure 7. The best fit values of the spectral indices  $\delta_1$  and  $\delta_2$  for every flaring event are shown.

the intrinsic spectrum falls as  $F_{\gamma,in} \propto E_{\gamma}^{-1}$  for  $E_{\gamma} > E_{\gamma}^c$ . In zone-1,  $F_{\gamma,in} \propto E_{\gamma}^{0.17}$ , a slowly increasing flux up to  $E_{\gamma}^c$ . In the photohadronic model we predict a mild peak-like structure at  $E_{\gamma}^c = 3.18$  TeV in the observed spectrum. On this day, the maximum observed photon energy was  $E_{\gamma} = 6.8$  TeV, corresponding to a minimum bulk Lorentz factor  $\Gamma \simeq 26.5$  which is consistent with the expectation from an EHBL. Except on 19th July, such spectral behavior was not observed on any other days. Also, such spectral behavior was not observed in the past from any of the HBLs, including Mrk 501.

It is to be noted that our two-zone photohadronic model explains extremely well all the 15 spectra of the VHE flaring events of Mrk 501. Other nearby HBLs, which have already shown the temporary EHBL-like behavior in the past, may reincarnate again with vigor and behave like the flaring of July 19, 2014 of Mrk 501 or even more complex. However, many more flaring events from nearby HBLs have to be studied to establish this claim. With the present and/or future generation of IACTs it will be possible to monitor such flaring events in great detail to better understand their emission mechanisms and enrich theoretical modeling.

The work of S.S. is partially supported by DGAPA-UNAM (Mexico) Project No. IN103522. A.U.P.O. and G. S.-C. would like to thank SECIHTI (Mexico) for partial support. Partial support from CSU-Long Beach is gratefully acknowledged. Pedro Fernández de Córdoba's work is partially supported by the Spanish government through the RD projects PID2021-128676OB-I00 and PID2022-142407NB-I00, as well as by the Excellence Research Groups Program of the Generalitat Valenciana, Spain (PROMETEO CIPROM/2023/32).

---

Abdalla, H., Aharonian, F., Ait Benkhali, F., et al. 2019, ApJ, 870, 93, doi: [10.3847/1538-4357/aaf1c4](https://doi.org/10.3847/1538-4357/aaf1c4)

Abdo, A. A., et al. 2009, ApJ, 700, 597

Abdo, A. A., Ackermann, M., Agudo, I., et al. 2010, ApJ, 716, 30, doi: [10.1088/0004-637X/716/1/30](https://doi.org/10.1088/0004-637X/716/1/30)

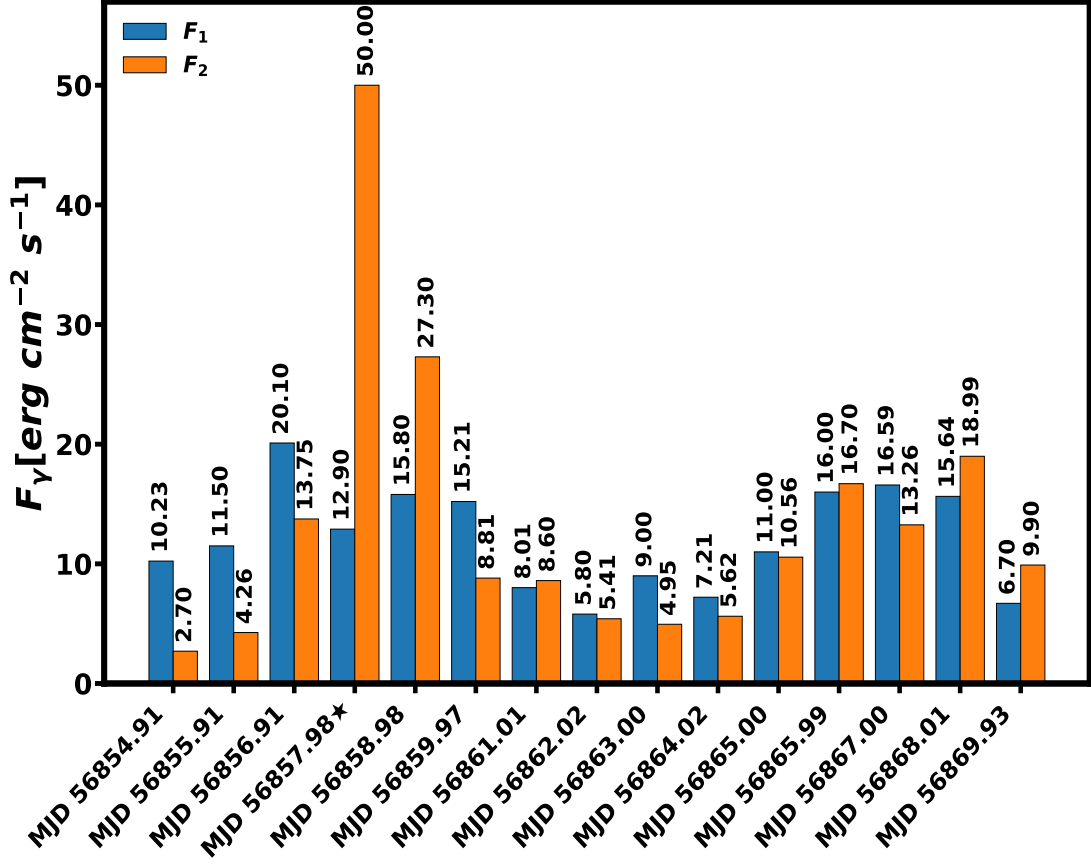


**Figure 8.** The best fit values of the normalization factors  $F_1$  and  $F_2$  in two-zone photohadronic model are shown for all the days.

Acciari, V., et al. 2019, MNRAS, 490, 2284

—. 2020, A&A, 638, A14

Ahnen, M., et al. 2017, A&A, 603, A31

—. 2018, A&A, 620, A181

Ahnen, M. L., Ansoldi, S., Antonelli, L. A., et al. 2018, A&A, 620, A181, doi: [10.1051/0004-6361/201833704](https://doi.org/10.1051/0004-6361/201833704)

Albert, J., et al. 2007, ApJ, 669, 862

—. 2008, ApJ, 681, 944

Aleksić, J., et al. 2015, A&A, 573, A50

Aliu, E., et al. 2016, A&A, 594, A76

Anderhub, H., Backes, M., Biland, A., et al. 2013, Journal of Instrumentation, 8, P06008, doi: [10.1088/1748-0221/8/06/P06008](https://doi.org/10.1088/1748-0221/8/06/P06008)

Biland, A., Bretz, T., Buß, J., et al. 2014, Journal of Instrumentation, 9, P10012, doi: [10.1088/1748-0221/9/10/P10012](https://doi.org/10.1088/1748-0221/9/10/P10012)

Boettcher, M., Reimer, A., Sweeney, K., & Prakash, A. 2013, ApJ, 768, 54, doi: [10.1088/0004-637X/768/1/54](https://doi.org/10.1088/0004-637X/768/1/54)

Böttcher, M., Dermer, C. D., & Finke, J. D. 2008, ApJL, 679, L9

Chandra, P., et al. 2017, NewA, 54, 42

Costamante, L., Bonnoli, G., Tavecchio, F., et al. 2018, MNRAS, 477, 4257

Costamante, L., et al. 2001, A&A, 371, 512

Dermer, C. D., & Schlickeiser, R. 1993, ApJ, 416, 458, doi: [10.1086/173251](https://doi.org/10.1086/173251)

Dermer, C. D., & Schlickeiser, R. 1993, ApJ, 416, 458

Dominguez, A., et al. 2011, MNRAS, 410, 2556

Dorner, D., Ahnen, M. L., Bergmann, M., et al. 2015, arXiv e-prints, arXiv:1502.02582, doi: [10.48550/arXiv.1502.02582](https://doi.org/10.48550/arXiv.1502.02582)

Foffano, L., Prandini, E., Franceschini, A., & Paiano, S. 2019, MNRAS, 486, 1741, doi: [10.1093/mnras/stz812](https://doi.org/10.1093/mnras/stz812)

Franceschini, A., Rodighiero, G., & Vaccari, M. 2008, A&A, 487, 837

Gehrels, N., Chincarini, G., Giommi, P., et al. 2004, ApJ, 611, 1005, doi: [10.1086/422091](https://doi.org/10.1086/422091)

Hu, W., & Yan, D. 2021, MNRAS, 508, 4038, doi: [10.1093/mnras/stab2442](https://doi.org/10.1093/mnras/stab2442)

Kataoka, J., et al. 1999, ApJ, 514, 138

- Kranich, D. 2009, arXiv e-prints, arXiv:0912.3830, doi: [10.48550/arXiv.0912.3830](https://doi.org/10.48550/arXiv.0912.3830)
- MAGIC Collaboration, Acciari, V. A., Ansoldi, S., et al. 2020, *A&A*, 637, A86, doi: [10.1051/0004-6361/201834603](https://doi.org/10.1051/0004-6361/201834603)
- Padovani, P., & Giommi, P. 1995, *ApJ*, 444, 567, doi: [10.1086/175631](https://doi.org/10.1086/175631)
- Paggi, A., Massaro, F., Vittorini, V., et al. 2009, *A&A*, 504, 821, doi: [10.1051/0004-6361/200912237](https://doi.org/10.1051/0004-6361/200912237)
- Petropoulou, M., Mastichiadis, A., Vasilopoulos, G., et al. 2024, *A&A*, 685, A110, doi: [10.1051/0004-6361/202347809](https://doi.org/10.1051/0004-6361/202347809)
- Petry, D., et al. 2000, *ApJ*, 536, 742
- Pian, E., Vacanti, G., Tagliaferri, G., et al. 1998, *ApJL*, 492, L17, doi: [10.1086/311083](https://doi.org/10.1086/311083)
- Pjanka, P., Zdziarski, A. A., & Sikora, M. 2017, *MNRAS*, 465, 3506, doi: [10.1093/mnras/stw2960](https://doi.org/10.1093/mnras/stw2960)
- Romero, G., Boettcher, M., Markoff, S., & Tavecchio, F. 2017, *SSRv*, 207, 5, doi: [10.1007/s11214-016-0328-2](https://doi.org/10.1007/s11214-016-0328-2)
- Sahu, S. 2019, *Rev. Mex. Fis.*, 65, 307
- Sahu, S., de León, A. R., & Nagataki, S. 2018, *EPJC*, 78, 484, doi: [10.1140/epjc/s10052-018-5954-2](https://doi.org/10.1140/epjc/s10052-018-5954-2)
- Sahu, S., de León, A. R., Nagataki, S., & Gupta, V. 2018, *EPJC*, 78, 557
- Sahu, S., López Fortín, C. E., Castañeda Hernández, L. H., Nagataki, S., & Rajpoot, S. 2020, *ApJ*, 901, 132, doi: [10.3847/1538-4357/abb089](https://doi.org/10.3847/1538-4357/abb089)
- Sahu, S., López Fortín, C. E., Castañeda Hernández, L. H., & Rajpoot, S. 2021a, *ApJ*, 906, 91, doi: [10.3847/1538-4357/abc9c6](https://doi.org/10.3847/1538-4357/abc9c6)
- Sahu, S., López Fortín, C. E., Iglesias Martínez, M. E., Nagataki, S., & Fernández de Córdoba, P. 2020, *MNRAS*, 492, 2261, doi: [10.1093/mnras/staa023](https://doi.org/10.1093/mnras/staa023)
- Sahu, S., López Fortín, C. E., Valadez Polanco, I. A., & Rajpoot, S. 2021b, *ApJ*, 914, 120, doi: [10.3847/1538-4357/abfd9a](https://doi.org/10.3847/1538-4357/abfd9a)
- Sahu, S., López Fortín, C. E., & Nagataki, S. 2019, *ApJL*, 884, L17
- Sahu, S., Miranda, L. S., & Rajpoot, S. 2016, *EPJC*, 76, 127, doi: [10.1140/epjc/s10052-016-3975-2](https://doi.org/10.1140/epjc/s10052-016-3975-2)
- Sahu, S., Osorio Oliveros, A. F., & Sanabria, J. C. 2013, *Phys. Rev. D*, 87, 103015, doi: [10.1103/PhysRevD.87.103015](https://doi.org/10.1103/PhysRevD.87.103015)
- Sahu, S., Yáñez, M. V. L., Miranda, L. S., de León, A. R., & Gupta, V. 2017, *EPJC*, 77, 18
- Tavecchio, F. 2014, *MNRAS*, 438, 3255
- Tavecchio, F., & Bonnoli, G. 2015, arXiv e-prints, arXiv:1512.05080, doi: [10.48550/arXiv.1512.05080](https://doi.org/10.48550/arXiv.1512.05080)
- Tavecchio, F., Maraschi, L., Pian, E., et al. 2001, *ApJ*, 554, 725, doi: [10.1086/321394](https://doi.org/10.1086/321394)
- Ulrich, M. H., Kinman, T. D., Lynds, C. R., Rieke, G. H., & Ekers, R. D. 1975, *ApJ*, 198, 261, doi: [10.1086/153603](https://doi.org/10.1086/153603)